Ceramics International 43 (2017) 476–483

Contents lists available at ScienceDirect

Ceramics International

journal homepage: www.elsevier.com/locate/ceramint

Surface effects on the degradation mechanism of bioactive PDMS-SiO_2-CaO-P_2O_5 hybrid materials intended for bone regeneration

D.A. Sánchez-Téllez[a,*], L. Téllez-Jurado[a], L.M. Rodríguez-Lorenzo[b,c], M.A. Mazo[d], J. Rubio[d], A. Tamayo[d,*]

[a] Instituto Politécnico Nacional-ESIQIE, Depto. de Ing. en Metalurgia y Materiales, UPALM-Zacatenco, 07738 Mexico City, Mexico
[b] Biomaterials Group, ICTP-CSIC, Juan de la Cierva, 3, 28006 Madrid, Spain
[c] Networking Biomedical Research Centre in Bioengineering, Biomaterials and Nanomedicine, CIBER-BBN, Spain
[d] Ceramics and Glass Institute, CSIC, Kelsen 5, 28049 Madrid, Spain

ARTICLE INFO

Keywords:
Degradation kinetics
Hybrid material
Apatite formation
Texture
Fractal

ABSTRACT

The purpose of this work is to study the dissolution mechanism of SiO_2-based bioactive hybrid materials containing both CaO and P_2O_5 in their structures and to determine the influence of apatite crystallization over the surface features of the hybrids during degradation. Hybrid materials were synthesized using *sol–gel* method. Tetraethoxysilane (TEOS), hydroxyl terminated polydimethylsiloxane (PDMS), $Ca(NO_3)_2{\cdot}4H_2O$, and triethyl phosphate (TEP) were used as reactants. The degradation and bioactivity of the hybrid materials were tested by soaking the specimens into simulated body fluid (SBF). Raman spectroscopy, tensiometry and N_2 adsorption/desorption curves were used to measure the changes during the degradation experiments. Several mathematical approaches have been taken to analyze the results. The growth of an apatite layer on the surface of SiO_2-modified PDMS-P_2O_5-CaO hybrid materials occurs together with degradation of the silica-based matrix. The dissolution kinetics depends upon the composition of the material. It varies from a surface-driven mechanism in the case of low-P_2O_5 samples to a degradation path which fits into a Weibull type kinetic model, typical of matrix dissolution processes in materials enriched in P_2O_5. During degradation, the surface parameters, fractal constant and anisotropy of the pores were determined. The slight increase of the fractal constant in low-containing P_2O_5 materials suggests the formation of a homogeneous silica-like layer in the first stage of degradation, which also works as anchoring nucleus for subsequent apatite formation. In all the cases, the degradation leads to ink-bottle shaped pores, increasing their volume as degradation occurs, but keeping their neck shape.

1. Introduction

The healing of critical size bone defects or low-quality bone fractures, as osteoporotic bones, requires longer times of healing than desired. And the longer healing times may result in several clinical complications. To prevent unforeseen difficulties, promising approaches, focused on the development of fixation devices that induce a simultaneous quick bone regeneration and material degradation while assuring enough mechanical properties to sustain the formation of the new functional tissue, are being studied [1–3].

Bioactive ceramics and bioactive glasses have attractive properties for bone repair and regeneration, such as osteointegration ability, and reasonable resorbability. They are capable of creating chemical bonds with the surrounding living tissue [4] thanks to the similarity of their chemical composition with that of natural bone. Nevertheless, organic-inorganic hybrid materials can be more attractive than ceramics and glasses since they are capable of overcoming some of the weaknesses of these materials, such as fragility or low mechanical resistance in bending. These hybrid materials are made of a combination of silica-based glasses with organic compounds chemically incorporated into the molecular structure of the vitreous silica [5]. The organic-inorganic hybrid materials can be synthesized through several approaches, being the *sol–gel* method the most widely used. This method is preferred due to its ability to tune the composition and texture of the biomaterials to fulfill the requirements of the final use.

One of the required properties for hybrid materials designed for bone regeneration is bioactivity, which is speculated to be the responsible for bone bonding [6]. Bioactivity is referred as the ability of the material to promote growth of a biologically active thin apatite layer on its surface [5,7,8]. This apatite-like layer, formed when the

* Corresponding authors.
E-mail addresses: danielatellez06@gmail.com (D.A. Sánchez-Téllez), aitanath@icv.csic.es (A. Tamayo).

http://dx.doi.org/10.1016/j.ceramint.2016.09.182
Received 8 June 2016; Received in revised form 21 September 2016; Accepted 26 September 2016
Available online 28 September 2016

material is soaked into physiological fluids during in vitro and in vivo assays, possesses a mineral composition very close to that of natural bones. It is also thought to be responsible for proteins adsorption, subsequent cell adhesion and proliferation and the ultimate success of the implant [9].

During in vitro bioactivity tests, soaking the materials into simulated body fluid (SBF), phosphate buffered saline (PBS) solution [1] or any physiological fluid, a first stage of surface dissolution and precipitation occurs [4]. The reactions in this stage involve surface ionic exchange between the ions in the hybrid and the ions contained in the fluids.

Several studies on bioactivity of biomaterials have been carried out focusing on *sol–gel* derived glasses and mesoporous silica [10–12]. However, the actual mechanisms of bioactivity-degradability are not yet well understood, but they seem to depend upon multiple factors including chemical composition, structure and/or modifications induced by the degradation kinetics of the biomaterials. In this context, the textural properties of the hybrid materials, such as porosity on surface, pore volume, pore size or pore structure play an important role on the behavior of the biomaterial. Although several authors have described the importance of these parameters when studying the biomaterials performance both on in vitro and on in vivo assays [6,7] it must to be taken into account that these textural properties and surface chemical composition vary continuously during the bioabsorption of these biomaterials. Kinetics of the apatite layer formation on the surface of the material goes hand in hand with the degradation rate process; so prior to implantation, it is important to ensure the structural stability of the biomaterial while the apatite grows, crystallizes and attaches to the surrounding tissue.

During bone regeneration, two competitive and simultaneous processes alter the surface of the material: apatite growth and biomaterial dissolution. Therefore, the physical, chemical and textural characteristics of the surface will be affected by the apatite precipitation and biomaterial dissolution processes [11,13]. It is generally accepted that when biodegradation begins, a first layer of carbonated apatite (c-AP) with Langmuir behavior is formed on the surface of the material. This c-AP may have two main functions: first, to act as a protective surface preventing the rapid corrosion of the material caused by the chemical attack of cations contained in the biological fluid and second, to serve as nucleation points for the growth of apatite-like species [10,14]. In CaO-containing silicates, the mechanism of apatite formation is described by an initial release of Ca^{2+} ions from their surfaces providing favorable sites for nucleation and crystallization of apatite. Then, the surfaces remaining are enriched in silanol groups which promote the formation of a hydrated amorphous silica gel layer through polycondensation reactions. At the same time, the release of Ca^{2+} ions increases the local super-saturation and enhances the ionic activity of the apatite in the solution [15]. A CaO-P_2O_5 film starts to precipitate onto the amorphous silica-rich layer due to the migration of Ca^{2+} and PO_4^{3-} ions from the material and the fluids. This coating grows with the incorporation of more Ca^{2+} and PO_4^{3-} ions from the solution. In a final stage, the CaO-P_2O_5 amorphous layer crystallizes into a carbonated apatite by the incorporation of CO_3^{2-} and OH^- [4,5,16].

Moreover, regarding to the degradation mechanism of a biomaterial, several mechanisms have been proposed [11]. The first mechanism involves the precipitation of a first layer of apatite in active spots located on the surface. These spots will be the nucleation points for the growth of more apatite on the surface. Out of these spots, the biomaterial is gradually dissolved according to its composition. A second mechanism involves an apatite layer covering the whole surface of the material. The dissolution will be directed by diffusion of the Si^{4+}, Ca^{2+} and PO_4^{3-} ions through the fresh layer and subsequent precipitation of apatite on the interphase barrier [10]. A third proposed mechanism implies the nucleation of a porous apatite layer covering the surface of the biomaterial. The migration of the cations will occur through the pores and the precipitation of a denser apatite layer will take place over the surface or the pore walls [10]. All the proposed mechanisms cause modifications in the textural characteristics of the materials surfaces. Therefore, the purpose of this work is to study the dissolution mechanism of SiO_2-based bioactive hybrid materials containing both CaO and P_2O_5 in their structures and to determine the influence of apatite crystallization over the surface features of the hybrids during degradation.

2. Materials and methods

2.1. Synthesis of the hybrid materials

Hybrid materials were synthesized using the *sol–gel* method as described elsewhere [1]. The solutions containing tetraethoxysilane (TEOS, $Si(OCH_2CH_3)_4$, Sigma-Aldrich), hydroxyl terminated polydimethylsiloxane (PDMS ($OH\text{-}[Si(CH_3)_2\text{-}O]_nH$, Sigma-Aldrich), CaO ($Ca(NO_3)_2{\cdot}4H_2O$, Fermont) and P_2O_5 (triethyl phosphate, TEP, $C_6H_{15}O_4P$, Sigma-Aldrich) were mixed in a flask at 80 °C under reflux and vigorous stirring. The weight ratio of PDMS/TEOS was maintained equal to 30/70 and CaO/TEOS was equal to 5 in all the cases. The weight ratio P_2O_5/TEOS was varied from 5 to 75. The obtained sols were poured into plastic containers and kept at room temperature for gelling and aging.

2.2. In vitro assays, degradability and bioactivity

The hydrolytic degradation and bioactivity of the hybrid materials dried at 100 °C were tested by soaking the specimens into 25 mL of simulated body fluid (SBF) at 36.5 °C and pH of 7.4. Four replica of each hybrid material were used. The SBF solution was prepared according to Kokubo's protocol [17]. The solution, having an ion concentration similar to blood plasma, was prepared by dissolving Na^+142.0, K^+5.0, Mg^{2+}1.5, Ca^{2+}2.5, Cl^- 147.8, HCO_3^- 4.2, HPO_4^{2-} 1.0, SO_4^{2-} 0.5 in deionized water and buffered at pH 7.4 with tris (hydroxymethyl) aminomethane (TRIS) and HCl 1N. The samples were soaked at intervals of 1, 3, 7, 14, 21, and 28 days and weighed after drying at 36.5 °C. The remaining SBF solution was collected after every soaking period and stored at 4 °C until analysis. The Si, Ca and P concentrations in the SBF solutions were determined through chemical analysis by inductively coupled plasma optical emission spectroscopy (ICP-OES, Iris Advantage, Thermo Jarrel Ash). At least five analyses were carried out from the filtered aliquots at each soaking time.

2.3. Characterization of the hybrid materials

Information about the structural characteristics of the surface of the materials was obtained by means of Raman spectroscopy. The samples were observed with a Leica LM/DM microscope which was also used to focus a 785 nm laser light to obtain a spot sized below 10 μm. At least 10 scans were collected in each 5 points randomly selected along the samples surfaces and the averaged spectra was plotted.

In order to evaluate the hydrophilic properties in the surface of the materials, the contact angle technique was used. The external angles formed between the water droplets and the surfaces of the materials were recorded. The measurements were made in a tensiometer CAM 200 KSV at room temperature, 23 °C. The equipment consists of a cam CCD with an optical telecentric zoom and with a stroboscopic light source. The automatic dispenser used is a drop precision Hamilton syringe of 1 mL with a needle of 0.71 mm in diameter. The contact angles were measured using digital photographs of 5 μL deionized water droplets in contact with the surface of the samples. Ten measurements, at different points, were made in each sample. The reported data is an average of the measurements and their corresponding standard deviation.

Adsorption/desorption analysis was carried out at 77 K using a

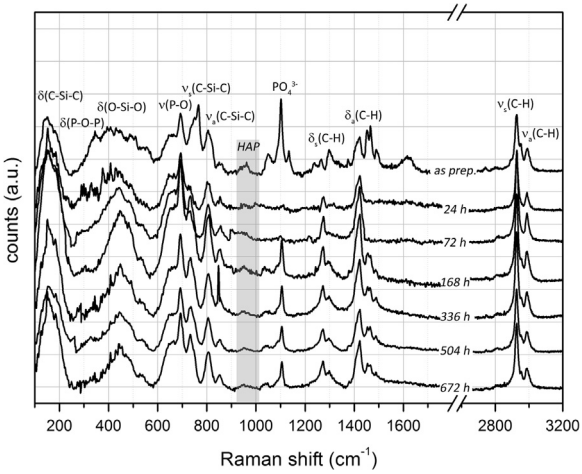

Fig. 1. Raman spectra of the hybrid materials (P_2O_5/TEOS=75) soaked for different periods of time. The shadowed area is centered on the most intense Raman band of HAP.

Tristar Micromeritics analyzer using nitrogen, N_2 (cross sectional area 0.164), as adsorptive gas. The samples were degassed under vacuum at 120 °C for 24 h prior to analysis. The adsorption–desorption curves provided data of the specific surface area, average pore size and pore volume in the materials. The surface area and pore-size distribution were determined by applying the model isotherm Brunauer-Emmett-Teller (BET) and the Barrett-Joyner-Halenda (BJH) method, respectively [18–20].

3. Results

3.1. Characterization of the apatite-like layer

The Raman spectra of the hybrid material with the composition of P_2O_5/TEOS=75 before and after being immersed in SBF are shown in Fig. 1. Similar Raman spectra were obtained for all the synthesized hybrid materials. The identified bands were assigned according to literature data [21,22] and their intensity depends on the amount of P_2O_5 and CaO within the hybrids and the period of time being immersed in the SBF solution. Several bands in the Raman spectra related to the silica-based hybrid materials are observed: the broad band located around 150 cm^{-1} is attributed to different configurations of the $Si(CH_3)_2$ groups in polydimethylsiloxane [21], whereas the vibration at~80 cm^{-1} correspond to the vibration modes assigned to ν(Si-O) stretching from the Si-O-R network, i.e. the ν_s(Si-O-Si). At higher Raman shifts, the stretching and bending vibrations of the C–H bonds of the PDMS network are located. It can be also detected a small and broad band centered near 962 cm^{-1}. This band can be assigned to the phosphate tetrahedron in hydroxyapatite, although the presence of phosphate within the structure of the material hampers the unambiguous assignation of this band. There are also several bands that are attributed to the phosphate ions, being the most representative the band near 695 cm^{-1}. This can be attributed to symmetric stretching mode of P-O-P from the bridging oxygen between the Q_3 phosphate tetrahedron.

The band observed at ~127 cm^{-1} may be attributed to the asymmetric stretching vibrations of PO_4 tetrahedron, specific for Q_2 species, and the asymmetric stretching of O-P-O (PO_2). As the P content

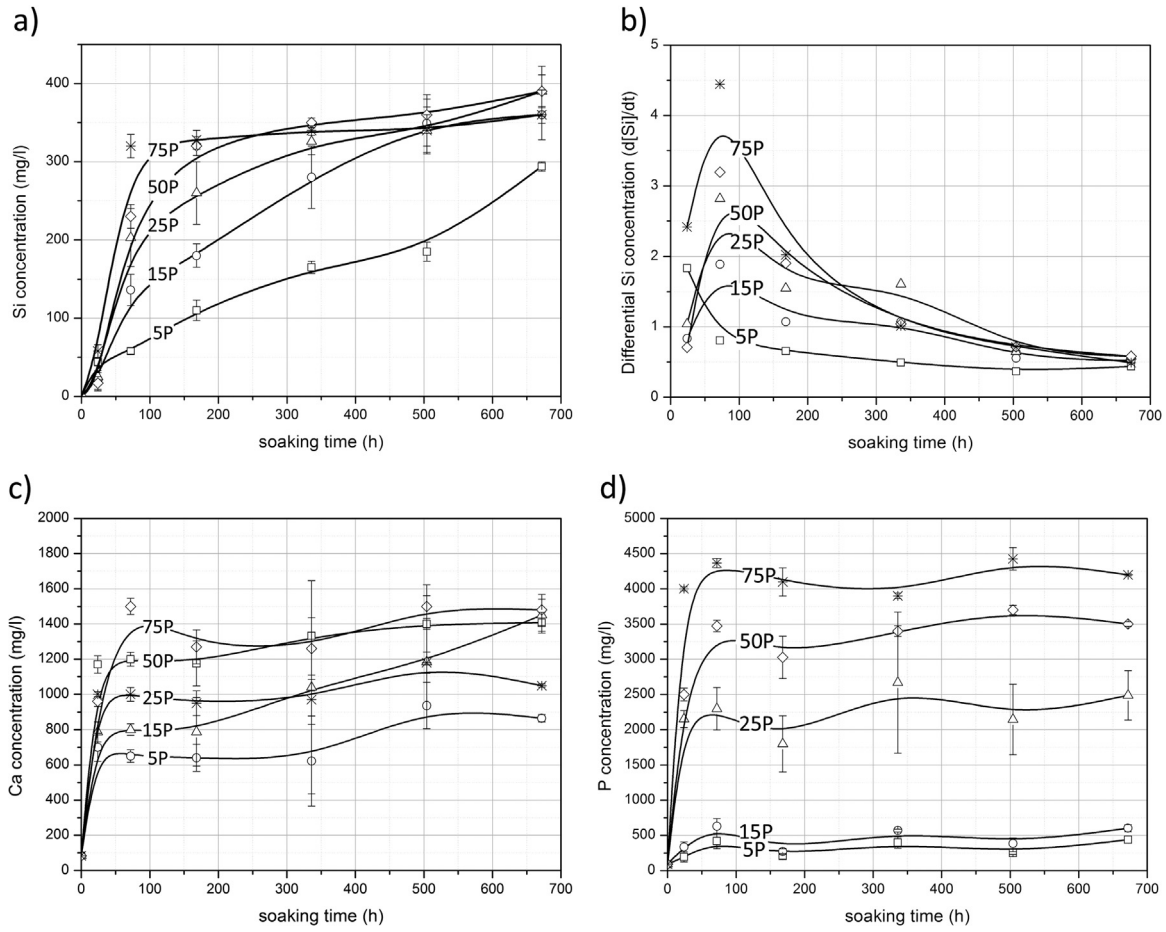

Fig. 2. a) Total amount and **b)** differential concentration of Si in the SBF solution after soaking periods of time. **c)** Total amount of Ca in the SBF solution after soaking periods of time. **d)** Total amount of P in the SBF solution after soaking periods of time.

increases, several other bands at ~740 and ~114 cm^{-1} also appear, being assigned to P-O-P bending in [PO_4] tetrahedron and the symmetric and stretching asymmetric vibration modes of Q_1 and Q_2 species, respectively.

3.2. Biodegradation studies

It has been determined the Si amount in the SBF solution after soaking the hybrid materials for the specified periods of time. As observed in Fig. 2a), the hybrid materials dissolved gradually according to its composition. Fig. 2b) reflects the differential curve of the Si concentration. It can be observed an initial burst in the solubility corresponding to 72 h in solution, a fact that occurs in all the cases except in the material with the lowest amount of P_2O_5. After a certain period of time, the Si coming from the hybrid materials was gradually leached. This initial burst is more pronounced when increasing the amount of P_2O_5 in the hybrid materials.

Regarding the total amount of Ca^{2+} and PO_4^{-3} released into SBF solution, the amount of Ca in the solution (Fig. 2c) increases 14-fold over the original amount in SBF, independently on the composition of the material and the soaking time. On the other hand, the released amount of P (Fig. 2d) varies with the composition but remains more or less invariable with the soaking time, indicating that equilibrium exists between the dissolution of the hybrid material and the apatite deposition.

Contact angle measurements in the as-prepared hybrid materials agree with the observed behavior (Table 1). The increase in P_2O_5 concentration reduces the intrinsic hydrophobic characteristic of the polydimethylsiloxane-based materials. The minor interconnectivity of the network induced by the P_2O_5 [1] leads to an increase of the Si-OH and P-OH groups within the hybrid structure and thus, the solubility of the materials is consequently enhanced. The presence of functional Si-OH and P-OH groups on the surface of the materials may attract water molecules by hydrogen bonding, leading to an increase in the hydrophilic properties of the materials.

The adsorption isotherms (Fig. 3a) of the hybrid materials with different P_2O_5 content show an increase in the porosity of the materials as the amount of P_2O_5increases. This is collected in Table 1, where the values of the specific surface areas calculated by application of the BET theory are shown. All the materials exhibit type IV isotherms, typical of mesoporous materials according to the IUPAC classification [20]. Fig. 3b presents the nitrogen adsorption-desorption isotherms of the material with the maximum amount of P_2O_5, before and after being soaked in SBF solution. The hysteresis loops, directly related to the mesopore volume, appear in all the materials soaked in the SBF, becoming more pronounced when both, P_2O_5 amount and soaking time increase.

The pore size distributions were calculated from the desorption branches of the isotherms by applying the BJH methodology [23]. As representative distributions, Fig. 3c presents the calculated PSDs of the as-prepared hybrid materials and Fig. 3d presents the corresponding ones obtained for the material with 5% P_2O_5 soaked in SBF for different periods of time. A maximum in the PSD near 3.4 nm can be detected. This maximum increases in intensity when the P amount and the soaking time increase. The materials with 25% and 50% P_2O_5 content also show a dual PSD with larger mesopores. Soaking exerts almost a lack of influence in these big sized mesopores, whose maxima in the PSD is ~2 nm in diameter.

Table 1
Contact angle and specific surface area (SBET) of the hybrid materials soaked in SBF.

P_2O_5/ TEOS	Contact angle	SBET (m^2/g)						
		0 h	24 h	72 h	168 h	336 h	504 h	672 h
5	146 ± 6	24	70	64	52	57	50	41
15	144 ± 7	46	50	72	35	29	31	42
25	135 ± 3	308	310	309	340	360	329	326
50	120 ± 5	264	646	339	327	291	252	297
75	92 ± 8	111	633	572	458	473	478	438

4. Discussion

The evolution of the structural characteristics in the hybrid materials along with the soaking periods was determined through the relative intensity of the Raman bands corresponding to the different groups of interest. Fig. 4 shows the relative intensity of the bands corresponding to the PO_4^{-3} ion, either from the added TEP during synthesis or the grown apatite during soaking time, in respect to the vibration of the Si-O-Si network, as a function of the soaking time. It is clearly observed that, in all the cases, after the third day of immersion, there is almost no difference between the relative intensities of the bands corresponding to the phosphate groups and the silica backbone. The relative intensity increases with the amount of P_2O_5 in the hybrid materials, except in the case of the material with the largest amount of P_2O_5. The stabilization of the intensity in the bands at longer periods of soaking time may confirm a constant composition in the materials' surfaces reached during the analysis.

The observed behavior is common in all the studied compositions, indicating that there is a limit in the growth of phosphate-rich species on the surface of the materials afterwards equilibrium is reached between HAP formation and material degradation. The degradation and release of Si^{4+}, Ca^{2+} and PO_4^{3-} ions occurs continuously during all the soaking period, creating a new porous texture into the materials, as revealed by the chemical analysis and nitrogen adsorption measurements. Nevertheless, the composition of the soaking solution with respect to Ca^{2+} and PO_4^{3-} remains invariable during all the soaking time, indicating that the dissolution and growth of a new surface layer occur simultaneously. The observed stabilization in the structural characteristics of the materials after 72 h of immersion in SBF solution suggests that once the c-AP layer is formed [14], the apatite growth on the surface occurs simultaneously with the degradation of the material matrix. This apatite growth, happening after 72 h, is related to the appearance of the band attributed to P–O–P bonds at ~740 and ~114 cm^{-1}, attributed to the [PO_4] tetrahedron and Q_1 and Q_2 units, respectively, which suggests the formation of different layers with different chemical structures.

To define the degradation mechanism of the hybrid materials soaked in SBF, mathematical approaches have been used to determine the kinetics of solubility. The amount of Si in solution is quantitatively analyzed by using model dependent methods based on different mathematical functions that describe the dissolution profiles. Fig. 2 shows a dissolution behavior typically found in biocompatible drug release systems. This behavior starts with an initial burst after a few hours of being soaked, followed by a steady state that lasts till the end of the experimental period.

Attempts to fit the experimental values into the established models indicate that degradation kinetics of each hybrid material should be described by using different models depending on their composition [24,25]. As observed in Fig. 2b, right after 24 h of immersion, the hybrid materials presented an initial large degradation before the release rate of Si reached a stable profile. This phenomenon is enhanced in the materials with the largest amount of P_2O_5. The solubility kinetics of the materials with P_2O_5 amounts exceeding 25% might fit the Weibull Model [24]. In this model, the amount of material released, M, is related with the leaching time, t, according to the following expression:

$$M = M_0(1 - e^{-kt}) \quad (1)$$

In this equation, the parameter k is a scale parameter that describes the time dependence and M_O is the total amount of leached material. Since the total amount of leached material is an unknown parameter,

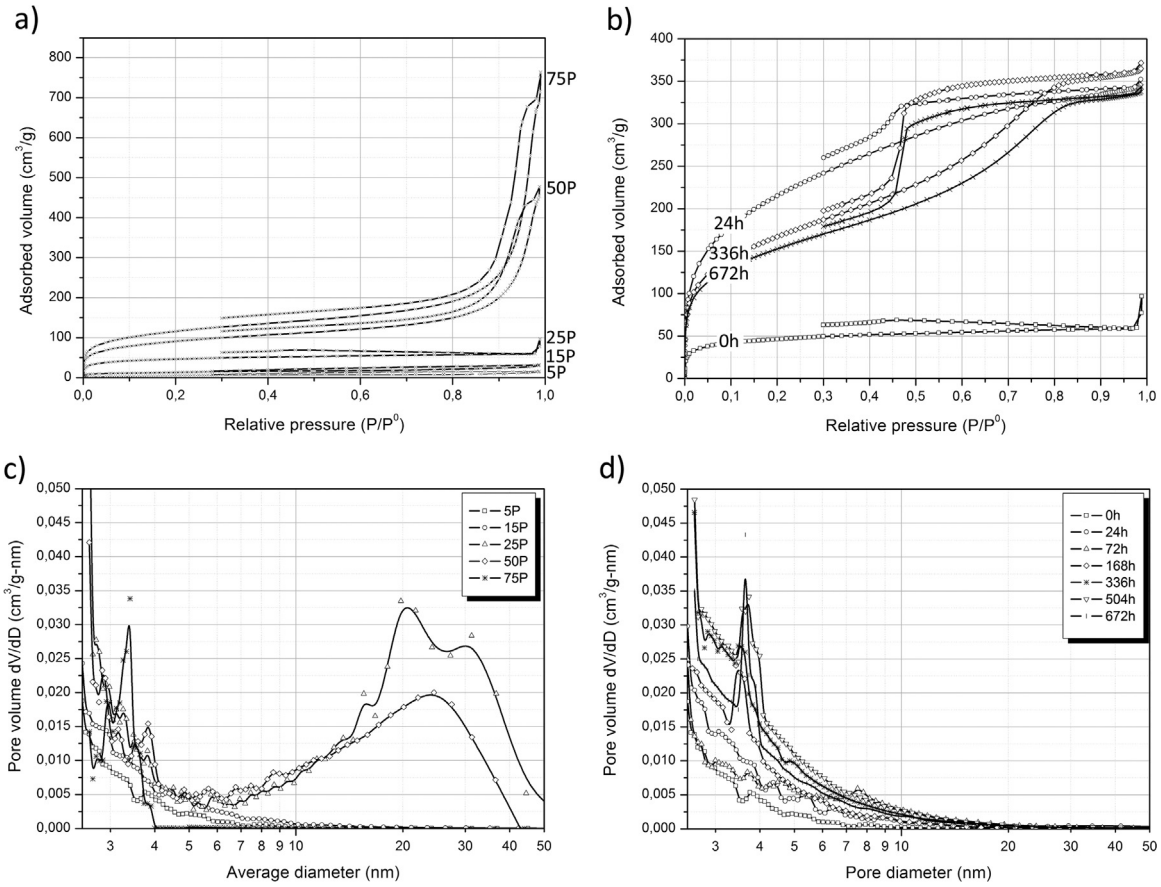

Fig. 3. Adsorption isotherms of **a)** the hybrid materials with different P_2O_5 amount and **b)** the hybrid material with P_2O_5/TEOS=75 soaked in SBF for different periods of time. Pore size distributions of **c)** the hybrid materials with different P_2O_5 amount and **d)** the hybrid material with P_2O_5/TEOS=5 soaked in SBF for different periods of time.

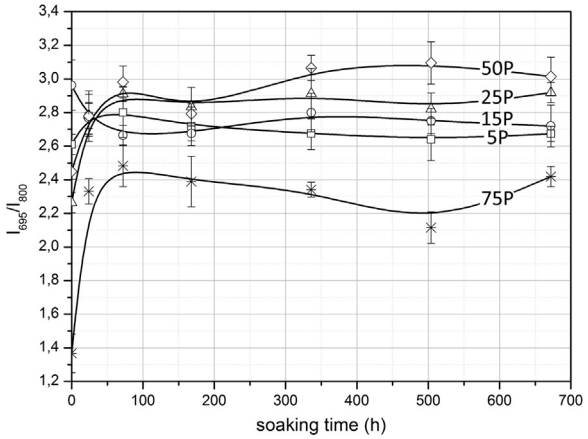

Fig. 4. Relative intensity of the Raman bands corresponding to the bending vibration modes of PO_4^{3-} (695 cm^{-1}) and Si-O-Si (800 cm^{-1}) of the hybrid materials as function of the soaking time.

Table 2
Dissolution kinetic fittings and kinetic parameters of the hybrid materials soaked in SBF.

P_2O_5/TEOS	Kinetic equation	Kinetic parameters	Correlation factor
5	$C = C_o e^{kt}$	$-4.38\ 10^{-2}$	0.96
15	$M^{1/3}-M_o^{1/3}=kt$	$-24.6\ 10^{-2}$	0.99
25		$-9.16\ 10^{-2}$	0.96
50	$M = M_0(1 - e^{-kt})$	$-10.2\ 10^{-2}$	0.95
75		$-6.48\ 10^{-2}$	0.96

this value was chosen to be the maximum amount of Si released (i.e., the amount of Si determined after 28 days of immersion in each hybrid material) as an approximation of the total amount of Si available for leaching in a reasonable time for a biodegradable material. The fitting parameters and the correlation coefficient obtained when comparing the experimental and fitted curves are collected in Table 2.

The Weibull Model, typical of matrix type dissolution processes, does not fit in the case of materials with fewer amounts of P_2O_5. In materials with 25% and 15% P_2O_5 content, the degradation is preferably directed by surface phenomena and its degradation kinetics can fit into the model proposed by Hixton and Crowell [24,25]. This model can be applied for those soluble materials that degrade in planes, parallel to the surface. The algebraic expression fitting this model is read as:

$$M^{1/3}-M_0^{1/3}=kt \quad (2)$$

Now, the parameter k may contain information about the surface–volume relation. In the case of the material with the less amount of P_2O_5 in its composition, the Si is leached following a first order kinetics, whose expression is given by:

$$C=C_0e^{kt} \quad (3)$$

Where C_O parameter is the initial concentration of drug, k parameter is the first order rate constant, and t parameter is the soaking time. This model is used to describe a solubility mechanism in which the material is hydrolytically degradable or is entrapped in an insoluble porous media [26]. The high hydrophobicity of the material, as determined by contact angle measurements, implies a lower Si^{4+} leaching rate. When the material is immersed in the SBF solution, a continuous silica layer is formed due to the chemical attack of the cations in the saline solution, resulting into a hydrophilic surface plenty of Si-OH and P-OH

groups.

The dissolution kinetics of each hybrid material was obtained by fitting the experimental values into mathematical models showing better levels of correlation of numerical adjustments, nevertheless it should be kept in mind that the comprehensive picture of the dissolution behavior cannot be only based on the fitting to one type of model or the other but instead, the dissolution kinetics of the material may present different degradation rates and degradation processes till it is completely dissolved. The dissolution mechanism may be therefore independent on the degradation kinetics.

It is well known that an amorphous silica-like layer is formed on the surface of the hybrid materials prior to apatite growth and crystallization, which acts as nucleation points for the heterogeneous nucleation of the biologically active carbonate apatite layer [11]. Whether the formation of this silica layer is a continuous process occurring during the degradation of the material or not, this must be determined by studying the surface characteristics of the material during the degradation process. The fractal parameters and pore characteristics of the surface imprints during the dissolution of hybrid materials containing SiO_2-CaO-P_2O_5 were thus determined to clarify the effect of the composition and surface properties on the bioreactivity and the mechanism of degradation process.

A thoughtful study of the data in the nitrogen adsorption-desorption isotherms allows to obtain accurate information about the surface characteristics of the hybrid materials. The method developed by Pfeifer and Avnir [27] deals with the use of the Frenkel-Halsey-Hill (FHH) adsorption isotherm, calculated from the N_2 adsorption measurements. The FHH isotherm consists on the representation of the volume of adsorbed N_2, V, at each partial pressure, P/P^O, according to the following expression [28]:

$$V=k\,(\ln P^0/P)^q \tag{4}$$

In this isotherm, K is a constant that depend on the adsorptive properties and q acquires a value that is related to the surface fractal dimension, D_s, which depends on the adsorption regime of the adsorbed N_2 [29]. The value of D_s is considered as a measure of the surface roughness. For smooth non-fractal surfaces, D_s=2, while for fractal surfaces $2 < D_s \leq 3$.

The nitrogen is adsorbed on the surface of the mesopores following three different stages. In the monolayer adsorption stage or van der Waals regime (vdW), all the adsorbed molecules are in contact with the surface of the material and thus the gas-solid interactions are dominant. In this case the factor q is related to D_s by means of:

$$q=(D_s-3)/3 \tag{5}$$

In the multilayer adsorption stage, more than one molecule are in direct contact with the surface of the material. The capillary condensation (CC) regime follows the multilayer adsorption stage, occurring when the gas condenses to a liquid-like phase in a pore at a certain pressure, P, lower than the saturation pressure of the bulk liquid. In this regime, the dominant forces controlling the adsorptive properties depend upon the surface tension of the liquid, and D_s is related to q as:

$$q=D_s-3 \tag{6}$$

The exact threshold between the different regimens is not always clear. In some cases, the adsorption adopts a configuration of a close-packed array of molecules in the monolayer, but in some others, the N_2 molecules may adopt a different structure. Thus, to determine which equation must be employed to calculate the correct D_s value, some authors have given an estimation of the limits where the vdW or CC equations must be applied [30]:

$$\omega=3(1+q)-2 \tag{7}$$

If $\omega > 0$, the wdW forces are dominant, while for $\omega < 0$ the liquid-gas surface tension forces are dominant.

The calculated surface fractal dimensions of the hybrid materials soaked in SBF presented similar D_s values, corresponding to *sol–gel*-derived materials [31,32] as shown in Fig. 5. In general, the fractal dimension exhibits a slight increase after 24 h of immersion in the materials with the lowest P_2O_5 content; however, the opposite occurs in materials with the highest P_2O_5 content. The D_s values remain more or less constant in all the materials after this period; though, the material with 5% P_2O_5 tends to acquire a smoother aspect, as interpreted from the minor fractal parameter. This material also presented a dissolution mechanism that could be fitted to a surface-dependent model..

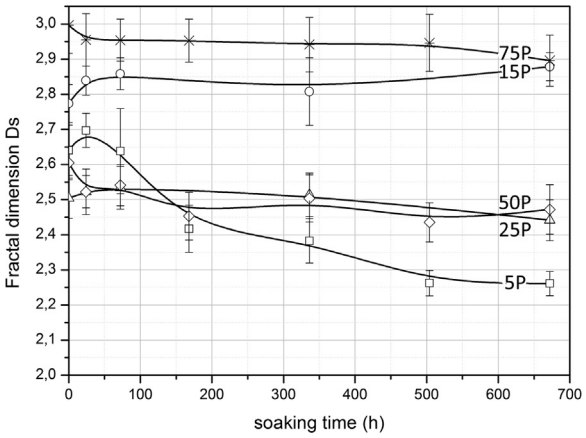

Fig. 5. Surface fractal dimension of the hybrid materials soaked in SBF.

The increase of the D_s value must be attributed to the formation of the above mentioned silica-like layer on the surface of the material after a few hours of immersion. The growth in D_s at low soaking times becomes less evident as the P_2O_5 amount increases, but the trend is reverted at the highest P_2O_5 concentrations. This fact is interpreted as follows: At low P_2O_5 concentration, the whole surface of the material is covered with the silica-like layer. On the other hand, the increase of P_2O_5 content hinders the formation of this layer, being formed only in some specific areas and acting as nucleation points for the formation of the apatite material. This statement agrees with the already reported behavior of the apatite growth, where it is mostly formed when the P_2O_5 concentration does not exceed 25 P_2O_5/TEOS [1].

It must be emphasized that the surface fractal parameter is strongly dependent upon the presence or absence of pores of different sizes. When comparing the different materials with different surface areas, it cannot be taken as a consideration the absolute values, but the observed trends within the same material when soaked in the SBF solution. Nevertheless, further information about the effect of the observed mesoporosity in the material's surface properties can be obtained by the application of the pore anisotropy model proposed by Pomonis and Armatas [33]. In this method, the pore anisotropy, b_i, of each group of i pores, can be estimated through the equation:

$$S_i^3/V_i^2=8\pi N_i r_i^{(\alpha_i-1)} \tag{8}$$

Being S_i and V_i the cumulative surface and volume of each group, respectively of N_i pores of radius r_i, and α_i being a scaling parameter whose determination allows the estimation of the pore anisotropy, b_i, which is expressed as a function of pore length, L_i, and pore diameter, D_i, as follows:

$$b_i=L_i/D_i=0.5 r_i^{\alpha_i-1} \tag{9}$$

Plots of $\log(S_i^3/V_i^2)$ vs $\log(r_i)$ allows the calculation of b_i through Eq. (9). As observed in Fig. 6, the anisotropy parameter, b_i, increases with soaking time, being more pronounced as P_2O_5 content increases within the composition of the materials. Taking into consideration the definition of b_i parameter, as described through Eq. (9), the length of pores would increase as the soaking time does, since, as shown in Fig. 3, the pore diameter remains constant despite the P_2O_5 concentration and soaking time.

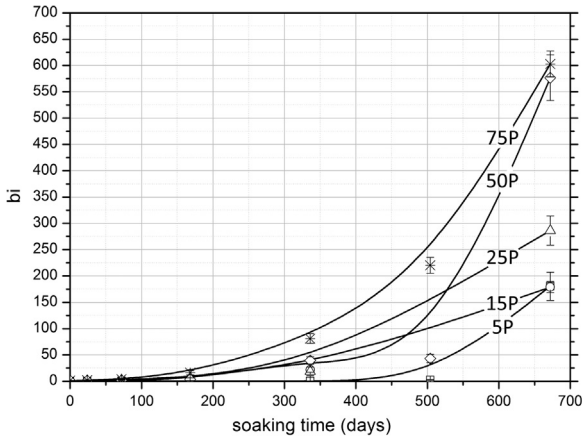

Fig. 6. Anisotropy parameter bi of the hybrid materials as function of the soaking time.

It must be clarified that the input used to obtain b_i parameter is related to pore volume and pore area, calculated through the application of the BJH methodology. This methodology uses the approximation of specified pore geometry, in the most simplified case, spherical pores are assumed. Considering the obtained values of b_i, the approximation for spherical pores is no longer valid; therefore, other pore geometry such as slit-shaped or cylindrical pores must be applied. For simplicity in the calculations, the same methodology in all the cases has been applied; but it is important to keep in mind that the obtained b_i values must not be taken as absolute values.

From the pore size distributions shown in Fig. 3 and the contribution of capillary condensation to the fractal parameter and the obtained values of b_i, it can be understood that degradation of the materials seems to occur in the form of ink-bottle shaped geometries, where the neck of the bottle remains more or less constant in diameter but its volume increases with both soaking time and P_2O_5 amount. The formation of these ink-bottle pores takes place despite of the silica-like layer covering the surface of the material after immersion in the SBF solution. This behavior must be related with the different phases formed on the materials surface after being soaked, i.e. the c-AP and amorphous silica layer.

Since the composition of the material surface remains almost unchanged after immersion, as revealed by comparison of the intensities corresponding to the phosphate ions and Si-O-Si bonds in the Raman spectra, the ink-bottle pores must be formed necessarily through the freshly formed apatite layer; otherwise, changes in the composition of the material surface would be expected. The more homogeneous the silica-like layer is, the smoother the apatite layer grows, the shorter the necks of the pores are and therefore, degradation is surface-dependent. On the other hand, spotted silica formation and heterogeneous nucleation in selected areas of P_2O_5-rich material lead to thicker apatite layers and deeper pore throws; therefore degradation kinetics can be explained by bulk-degradation mechanisms.

5. Conclusions

SiO_2-modified PDMS-P_2O_5-CaO hybrids are proven to be highly bioactive materials in terms of apatite growth. Degradation of the hybrids occurs simultaneously to the apatite growing. The degradation kinetics depends upon the composition of the material: A surface-driven mechanism is observed for low-P_2O_5 containing specimens whereas a matrix dissolution driven process is prevalent for materials enriched in P_2O_5. The porous texture of the hybrids surfaces suffered significant changes during immersion. Apatite crystallization depends on P_2O_5 content. In P_2O_5-rich hybrids, the formation of the amorphous silica-like layer is hindered; therefore, the growth of an apatite layer is hindered too. Although, pores seem to acquire the geometry of an ink-bottle shape in any case, the pore volume increases with the P_2O_5 content. Thus, for greater apatite crystallization, lower pore volume in the hybrids is obtained.

Acknowledgments

This work was supported by SIP-IPN 20150064 Project (Mexico), DGICYT Project, MAT2014-51918-C2-1-R (Spain), Fundación General CSIC (Programa ComFuturo) (A. Tamayo). DA Sánchez – Téllez also acknowledges CONACYT for the scholarship given.

References

[1] D.A. Sanchez-Tellez, L. Tellez-Jurado, L.M. Rodriguez-Lorenzo, Optimization of the CaO and P2O5 contents on PDMS-SiO2-CaO-P2O5 hybrids intended for bone regeneration, J. Mater. Sci. 50 (2015) 5993–6006.
[2] P.V. Giannoudis, I. Pountos, Tissue regeneration: the past, the present and the future, Injury 36 (2005) S2–S5.
[3] G. Zhao, O. Zinger, Z. Schwartz, M. Wieland, D. Landolt, B.D. Boyan, Osteoblast-like cells are sensitive to submicron-scale surface structure, Clin. Oral Implant. Res. 17 (2006) 258–264.
[4] M. Mozafari, F. Moztarzadeh, M. Tahriri, Investigation of the physico-chemical reactivity of a mesoporous bioactive SiO2-CaO-P2O5 glass in simulated body fluid, J. Non-Cryst. Solids 356 (2010) 1470–1478.
[5] L.M. Rodriguez-Lorenzo, Apatite: synthesis, in: M. Iafisco, J.M. Delgado-Lopez (Eds.), Structural Characterization and Biomedical Applications, Nova Science Publishers, New York, 2014.
[6] M. Mami, A. Lucas-Girot, H. Oudadesse, R. Dorbez-Sridi, F. Mezahi, E. Dietrich, Investigation of the surface reactivity of a solâ€“gel derived glass in the ternary system SiO2-CaO-P2O5, Appl. Surf. Sci. 254 (2008) 7386–7393.
[7] N.LetaïefA.Lucas-GirotH.OudadesseR.Dorbez-SridiP.Boullay, Investigation of the surfactant type effect on characteristics and bioactivity of new mesoporous bioactive glass in the ternary system SiO_2-CaO-P_2O_5: structural, textural and reactivity studies, Microporous Mesoporous Mater. vol.195, pp.102–111.
[8] S.V. Dorozhkin, Bioceramics of calcium orthophosphates, Biomaterials 31 (2010) 1465–1485.
[9] V. Aina, C. Morterra, G. Lusvardi, et al., Ga-modified (Si-Ca-P) Sol–Gel glasses: possible relationships between surface chemical properties and bioactivity, J. Phys. Chem. C 115 (2011) 22461–22474.
[10] S.B. Park, Y.-H. Joo, H. Kim, W. Ryu, Park Y-i, Biodegradation-tunable mesoporous silica nanorods for controlled drug delivery, Mater. Sci. Eng.: C 50 (2015) 64–73.
[11] Q. He, J. Shi, M. Zhu, Y. Chen, F. Chen, The three-stage in vitro degradation behavior of mesoporous silica in simulated body fluid, Microporous Mesoporous Mater. 131 (2010) 314–320.
[12] A. Kunzmann, B. Andersson, T. Thurnherr, H. Krug, A. Scheynius, B. Fadeel, Toxicology of engineered nanomaterials: Focus on biocompatibility, biodistribution and biodegradation, Biochim. Biophys. Acta (BBA) – (Gen. Subj.) 1810 (2011) 361–373.
[13] K.K. Pohaku Mitchell, A. Liberman, A.C. Kummel, W.C. Trogler, Iron(III)-doped, silica Nanoshells: a biodegradable form of silica, J. Am. Chem. Soc. 134 (2012) 13997–14003.
[14] S. Radin, S. Falaize, M.H. Lee, P. Ducheyne, In vitro bioactivity and degradation behavior of silica xerogels intended as controlled release materials, Biomaterials 23 (2002) 3113–3122.
[15] S. Ni, K. Lin, J. Chang, L. Chou, β-CaSiO3/β-Ca3(PO4)2 composite materials for hard tissue repair: in vitro studies, J. Biomed. Mater. Res. Part A 85A (2008) 72–82.
[16] N. Zhang, J.A. Molenda, J.H. Fournelle, W.L. Murphy, N. Sahai, Effects of pseudowollastonite (CaSiO3) bioceramic on in vitro activity of human mesenchymal stem cells, Biomaterials 31 (2010) 7653–7665.
[17] T. Kokubo, H. Kushitani, C. Ohtsuki, S. Sakka, T. Yamamuro, Effects of ions dissolved from bioactive glass-ceramic on surface apatite formation, J. Mater. Sci.-Mater. Med. 4 (1993) 1–4.
[18] S.J.GreggK.S.W.Sing, Academic Press, London, 1982.
[19] K.S.W. Sing, D.H. Everett, R.A.W. Haul, et al., Reporting physisorption data for gas solid systems with special reference to the determination of surface area and porosity (recommendations 1984), Pure Appl. Chem. 57 (1985) 603–619.
[20] M. Thommes, K. Kaneko, A.V. Neimark, et al., Physisorption of gases, with special reference to the evaluation of surface area and pore size distribution (IUPAC technical report), Pure Appl. Chem. 87 (2015) 1051–1069.
[21] A. Tamayo, J. Rubio, Structure modification by solvent addition into TEOS/PDMS hybrid materials, J. Non-Cryst. Solids 356 (2010) 1742–1748.
[22] P.N. de Aza, F. GuitiÃin, C. Santos, S. de Aza, R. CuscÃ³, L. ArtÃºs, Vibrational properties of calcium phosphate compounds. 2. comparison between hydroxyapatite and Î²-Tricalcium Phosphate, Chem. Mater. 9 (1997) 916–922.
[23] E.P. Barrett, L.G. Joyner, P.P. Halenda, The determination of pore volume and area distributions in porous substances. I. computations from nitrogen isotherms, J. Am. Chem. Soc. 73 (1951) 373–380.
[24] S. Dash, P.N. Murthy, L. Nath, P. Chowdhury, Kinetic modeling on drug release from controlled drug delivery systems, Acta Pol. Pharm. 67 (2010) 217–223.
[25] J. Siepmann, F. Siepmann, Mathematical modeling of drug dissolution, Int. J. Pharm. 453 (2013) 12–24.

[26] A.R. Tzafriri, Mathematical modeling of diffusion-mediated release from bulk degrading matrices, J. Control. Release 63 (2000) 69–79.
[27] D. Avnir, D. Farin, P. Pfeifer, Chemistry in noninteger dimensions between 2 and 3.2. fractal surfaces of adsorbents, J. Chem. Phys. 79 (1983) 3566–3571.
[28] P.J. Pomonis, E.T. Tsaousi, Frenkel-Halsey-Hill equation, dimensionality of adsorption, and pore anisotropy, Langmuir 25 (2009) 9986–9994.
[29] F. Rubio, J. Rubio, J.L. Oteo, Effect of heating on the surface fractal dimensions of ZrO2, J. Mater. Sci. Lett. 16 (1997) 49–52.
[30] I.M.K. Ismail, P. Pfeifer, Fractal analysis and surface roughness of non porous carbon fibers and carbon blacks, Langmuir 10 (1994) 1532–1538.
[31] A. Tamayo, L. Tellez, M. Rodriguez-Reyes, M.A. Mazo, F. Rubio, J. Rubio, Surface properties of bioactive TEOS-PDMS-TiO2-CaO ormosils, J. Mater. Sci. 49 (2014) 4656–4669.
[32] J. Mrowiec-BiaÅ, oÅ, L. PajaÌ§k, A.B. JarzeÌ§bski, A.I. Lachowski, J.J. Malinowski, Morphology of silica aerogels obtained from the process catalyzed by NH4F and NH4OH, Langmuir 13 (1997) 6310–6314.
[33] P.J. Pomonis, G.S. Armatas, A method for the estimation of pore anisotropy in porous solids, Langmuir 20 (2004) 6719–6726.